4-1-2020

Dietary Choline Supplementation Attenuates High-Fat-Diet-Induced Hepatocellular Carcinoma in Mice

Amanda L. Brown
Cleveland Clinic Foundation

Kelsey Conrad
University of Cincinnati College of Medicine, kconrad@smith.edu

Daniela S. Allende
Cleveland Clinic Foundation

Anthony D. Gromovsky
Cleveland Clinic Foundation

Renliang Zhang
Cleveland Clinic Foundation

See next page for additional authors

The Journal of Nutrition
Nutrient Physiology, Metabolism, and Nutrient-Nutrient Interactions

Dietary Choline Supplementation Attenuates High-Fat-Diet–Induced Hepatocellular Carcinoma in Mice

Amanda L Brown,[1] Kelsey Conrad,[2] Daniela S Allende,[3] Anthony D Gromovsky,[1] Renliang Zhang,[1] Chase K Neumann,[1] A Phillip Owens, III,[2] Michael Tranter,[2] and Robert N Helsley[1,2]

[1]Department of Cardiovascular and Metabolic Sciences, Lerner Research Institute, Cleveland Clinic, Cleveland, OH, USA; [2]Division of Cardiovascular Health and Disease, Department of Internal Medicine, University of Cincinnati College of Medicine, Cincinnati, OH, USA; and [3]Department of Pathology, Pathology and Laboratory Medicine Institute, Cleveland Clinic, Cleveland, OH, USA

ABSTRACT

Background: Hepatocellular carcinoma (HCC) is the third most common cause of cancer-related death in the world. Choline deficiency has been well studied in the context of liver disease; however, less is known about the effects of choline supplementation in HCC.

Objective: The objective of this study was to test whether choline supplementation could influence the progression of HCC in a high-fat-diet (HFD)–driven mouse model.

Methods: Four-day-old male C57BL/6J mice were treated with the chemical carcinogen, 7,12-dimethylbenz[a]anthracene, and were randomly assigned at weaning to a cohort fed an HFD (60% kcal fat) or an HFD with supplemental choline (60% kcal fat, 1.2% choline; HFD+C) for 30 wk. Blood was isolated at 15 and 30 wk to measure immune cells by flow cytometry, and glucose-tolerance tests were performed 2 wk prior to killing. Overall tumor burden was quantified, hepatic lipids were measured enzymatically, and phosphatidylcholine species were measured by targeted MS methods. Gene expression and mitochondrial DNA were quantified by quantitative PCR.

Results: HFD+C mice exhibited a 50–90% increase in both circulating choline and betaine concentrations in the fed state ($P \leq 0.05$). Choline supplementation resulted in a 55% decrease in total tumor numbers, a 67% decrease in tumor surface area, and a 50% decrease in hepatic steatosis after 30 wk of diet ($P \leq 0.05$). Choline supplementation increased the abundance of mitochondria and the relative expression of β-oxidation genes by 21% and ~75–100%, respectively, in the liver. HFD+C attenuated circulating myeloid-derived suppressor cells at 15 wk of feeding ($P \leq 0.05$).

Conclusions: Choline supplementation attenuated HFD-induced HCC and hepatic steatosis in male C57BL/6J mice. These results suggest a therapeutic benefit of choline supplementation in blunting HCC progression. *J Nutr* 2020;150:775–783.

Keywords: hepatocellular carcinoma, nonalcoholic fatty liver disease, choline, myeloid-derived suppressor cells, high-fat diet

Introduction

Liver cancer is a leading cause of cancer death in the United States and worldwide, accounting for nearly 800,000 deaths in 2018 (1). Hepatocellular carcinoma (HCC) is the most common type of primary liver cancer (2) and the incidence of HCC continues to increase, with an overall 5-y survival rate of <15% (3). HCC is primarily caused by cirrhosis of the liver, with ~80% of HCC cases occurring in patients with cirrhosis resulting from viral hepatitis infection and nonalcoholic fatty liver disease (NAFLD) (2). HCC is a progressive disease, and although liver resection, liver transplant, and tumor ablation are considered curative treatment options at different stages of disease, ~70% of HCC patients experience tumor recurrence within 5 y (4). Treatment options for patients with recurrent and advanced-stage HCC are scarce and drug development for the treatment of advanced disease has shown little success (3); thus, elucidating the mechanisms contributing to HCC progression and identifying potential drug targets from these studies remain a priority.

Choline is an essential nutrient obtained through dietary sources and derived from the de-novo synthesis of phosphatidylcholine (PC) in the liver (5). Choline and its metabolites perform a wide range of physiological and metabolic functions. PC constitutes 40–50% of cell membranes and 70–95% of phospholipids in lipoproteins, surfactant, and bile (6). Choline is necessary for the formation of the neurotransmitter acetylcholine, and the choline metabolite betaine is needed for

Manuscript received November 5, 2019. Initial review completed November 21, 2019. Revision accepted November 26, 2019.
First published online December 18, 2019; doi: https://doi.org/10.1093/jn/nxz315.

normal kidney glomerular function, mitochondrial function, and methylation reactions (6).

In the liver, PC is required for the synthesis of VLDL, which package and secrete triglycerides from the liver (6). Insufficient PC prevents the secretion of triglycerides and leads to lipid deposition in the liver (6). NAFLD can develop and progress to cirrhosis, increasing the risk of HCC. In rodents, it is well documented that low dietary choline intake is a risk factor for NAFLD and HCC (7–9). In an early study, rats fed a choline-deficient diet for 52 wk developed significant fatty liver with a 15% incidence of HCC (7). Similarly, rats fed a choline-methionine–deficient diet for 24 mo exhibited a 51% incidence of HCC (8).

In humans, the association between choline deficiency and progressive fatty liver disease is exemplified in patients receiving prolonged total parenteral nutrition (TPN). Plasma choline is low in up to 84% of patients receiving TPN (5, 10). These patients exhibit hepatic steatosis and liver damage, which can be resolved with choline supplementation (10). Although it is well established that choline deficiency contributes to progressive fatty liver disease in humans and rodents, it remains unclear whether choline supplementation in the absence of choline deficiency could be protective against the development of HCC. Our results suggest that supplemental dietary choline may be a viable therapeutic against HCC.

Methods

Animals, diets, and experimental design

Male C57BL/6J mice were purchased from Jackson Laboratories (stock #000664). 7,12-Dimethylbenz[*a*]anthracene (DMBA) treatments were performed using a previous protocol (11). Briefly, a single 50-μL application of a 0.5% DMBA (D3254; Sigma-Aldrich) solution in acetone was applied to the dorsal surface of mice 4 d after birth (11). Mice were weaned at 21 d, then were fed either a high-fat diet (HFD; 60% kcal fat; D12492; Research Diets, Inc.) or an HFD with 1.2% choline (HFD+C; 60% kcal fat; D15100402; Research Diets, Inc.) for 30 wk. In this model, mice will only develop HCC if fed an HFD in combination with DMBA (11, 12). The D12492 base diet, mineral mix (S10026; Research Diets, Inc), and vitamin mix (V10001; Research Diets, Inc.) have all been described previously (13). The HFD+C is the base diet supplemented with choline at 1.2%, which is ∼9.6 times more choline than the control HFD. All mice were maintained in an Association for the Assessment and Accreditation of Laboratory Animal Care International–approved animal facility, and all experimental protocols were approved by the Institutional Animal Care and Use Committee at the Cleveland Clinic.

Supported by a grant provided by the American Heart Association to RNH (17POST32850000).
Author disclosures: The authors report no conflicts of interest.
Supplemental Figures 1–5 and Supplemental Tables 1 and 2 are available from the "Supplementary data" link in the online posting of the article and from the same link in the online table of contents at https://academic.oup.com/jn/.
ALB and KC are co–first authors.
Abbreviations used: *Acox1*, acyl-CoA oxidase 1; ALT, alanine aminotransferase; AST, aspartate aminotransferase; *Cpt1a*, carnitine palmitoyltransferase 1A; DMBA, 7,12-dimethylbenz[a]anthracene; HCC, hepatocellular carcinoma; HFD, high-fat diet; HFD+C, high-fat diet with supplemental choline; *Hmgcr*, 3-hydroxy-3-methyl-glutaryl-coenzyme A reductase; LC/ESI/MS/MS, liquid chromatography electrospray ionization tandem-MS; *Ldlr*, LDL receptor; MDSC, myeloid-derived suppressor cell; NAFLD, nonalcoholic fatty liver disease; PC, phosphatidylcholine; *Ppar*, peroxisome proliferator-activated receptor; *Slc44a1*, solute carrier family 44 member 1; *Srebp*, sterol response element binding protein; SRM, Selected Reaction Monitoring; TPN, total parenteral nutrition.
Address correspondence to RNH (e-mail: roberthelsley07@gmail.com).

Standardized necropsy conditions

All experimental mice were feed-deprived for 4 h (from 09:00 to 13:00 h) prior to necropsy. At necropsy, all mice were terminally anesthetized with ketamine/xylazine (100–160 mg/kg ketamine; 20–32 mg/kg xylazine), and a midline laparotomy was performed. Blood was collected from the left ventricle via cardiac puncture, followed by whole-body perfusion with 10 mL of 0.9% saline into the heart and out through a puncture in the inferior vena cava. Tissues were collected and either fixed for morphological analysis or immediately snap-frozen in liquid nitrogen for subsequent biochemical analysis.

Measurement of circulating choline and betaine concentrations

Mouse plasma aliquots were used to measure plasma choline and betaine concentrations as previously described (14, 15). Choline and betaine were quantified with the use of a stable-isotope-dilution assay and HPLC with on-line electrospray ionization tandem-MS (LC/ESI/MS/MS) on an AB SCIEX QTRAP5500 mass spectrometer; d4(1,1,2,2,)-choline was used as an internal standard (14, 15).

Intraperitoneal glucose-tolerance test

Glucose-tolerance tests were performed as previously described (16–18). Briefly, mice were injected with glucose at 2 g/kg body weight into the peritoneal cavity. Tail-vein plasma glucose concentrations were measured using a commercial glucometer (ACCU-CHEK Performa; Roche).

Liver histology

Hematoxylin and eosin staining of formalin-fixed and paraffin-embedded liver sections was performed as described previously (17, 18). Pathological analysis was completed by a blinded board-certified pathologist (DSA) at the Cleveland Clinic.

Hepatic cholesterol and triglyceride analyses

Quantification of total hepatic triglycerides, total cholesterol, and free cholesterol was conducted using enzymatic assays as described previously (16–19). Extraction of the liver lipids was completed using a previous protocol (19). The extracted lipids were then quantified using the following enzymatic assays: triglycerides (L-Type Triglyceride M; Wako Diagnostics), total cholesterol (ThermoScientific™ Total Cholesterol Reagents), and free cholesterol (Cholesterol E; Wako Diagnostics). Esterified cholesterol is quantified by subtracting the free cholesterol from the total cholesterol.

Relative quantitation of PC lipids

A targeted lipidomic assay for PC lipids was developed using HPLC on-line LC/ESI/MS/MS. A total of 40 PC lipids (from PC-28:0 to PC-44:4) in liver tissue homogenates were analyzed by this method.

Standard solutions.

The standard, PC-36:0, and the internal standard, PC-33:1-d7, were used to generate the internal standard curve for calibration of all the PC lipids. Both were purchased from Avanti Polar Lipids. Standard PC-36:0 solution at concentrations of 0, 10, 50, 200, 1000, 5000, and 20,000 ng/mL were prepared in 80% methanol containing the internal standard at the concentration of 500 ng/mL. The volume of 5 μL was injected into the Vanquish UHPLC system (Thermo Fisher Scientific).

Lipid extraction.

Total hepatic lipids were extracted using a previously described method (18).

HPLC parameters.

A C18 column (2.1 × 150 mm, Gemini, 3 μm; Phenomenex) was used for the separation of PC lipids. Mobile phases were A (water containing 0.2% ammonium hydroxide) and B [methanol/acetonitrile, 1/1 (vol/vol) containing 0.2% ammonium hydroxide]. Mobile phase B at 80% was used from 0 to 2 min at the flow rate of 0.3 mL/min and then a linear

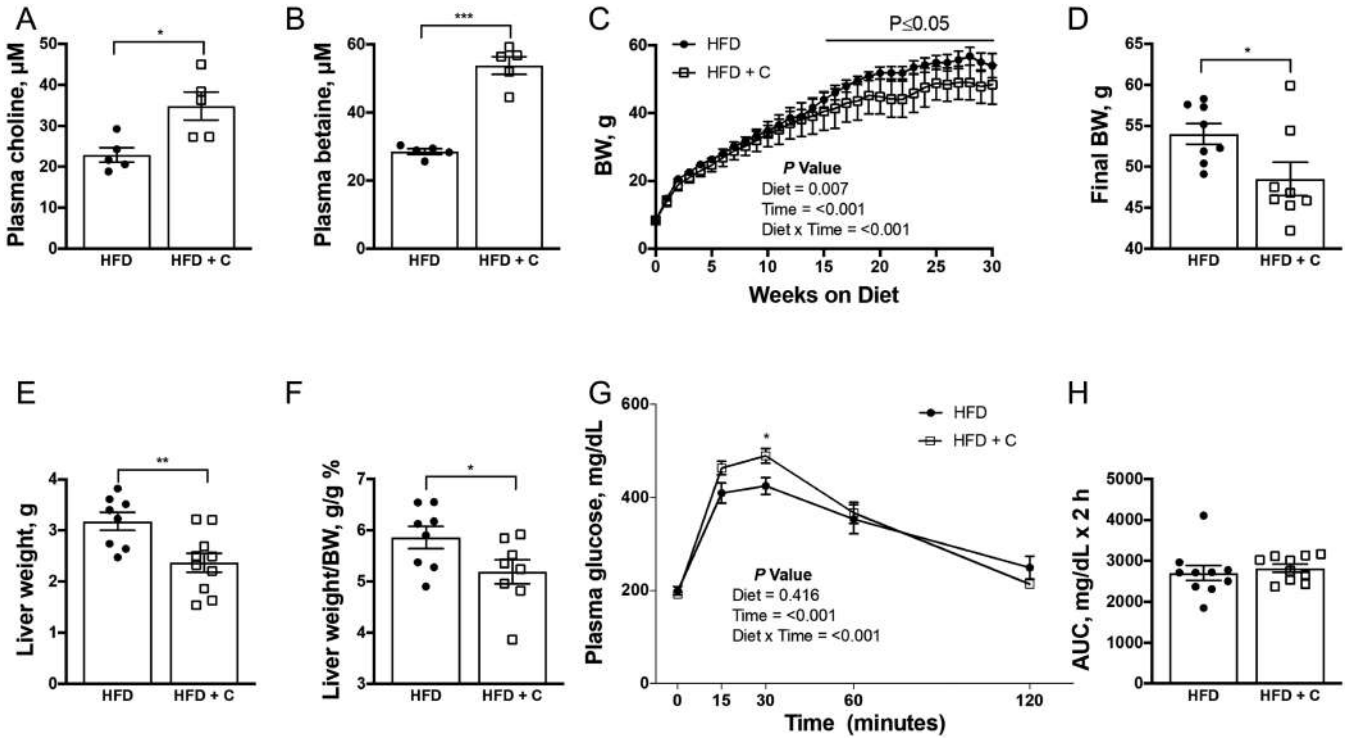

FIGURE 1 Dietary choline supplementation reduces overall body and liver weights in mice fed an HFD. Plasma choline (A) and betaine (B) concentrations in fed mice at 15 wk of feeding ($n = 5$). Body weights throughout the study (C), at the end of the study (D), absolute (E) and relative (F) liver weights, and glucose measured during an IPGTT (G) and the IPGTT AUC (H) in mice fed an HFD or an HFD+C ($n = 7$–10) are shown. All data are presented as means ± SEMs. A 2-tailed Student's *t* test was used in panels A, B, E, and F. A Mann–Whitney rank sum test was used in panels D and H. A repeated-measures 2-factor ANOVA with Holm–Sidak post-hoc analysis was used for panels C and G. $^{*}P \leq 0.05$; $^{**}P \leq 0.01$; $^{***}P \leq 0.001$. BW, body weight; HFD, high-fat diet; HFD+C, high-fat diet with supplemental choline; IPGTT, intraperitoneal glucose-tolerance test.

gradient from 80% B to 100% B from 2 to 8 min, maintained at 100% B from 8 to 20 min, then 100% B to 80% B from 20 to 20.1 min, and maintained at 80% B from 20.1 to 29 min.

Mass spectrometer parameters.

The HPLC eluent was directly injected into a triple-quadrupole mass spectrometer (TSQ Quantiva; Thermo Fisher Scientific) and the PC lipids were ionized at the positive mode. PC lipids were monitored using Selected Reaction Monitoring (SRM) and the SRM transitions were the *m/z* of molecular cation of each PC to the daughter ion *m/z* 184, the specific phosphocholine group.

Data analysis.

The software Xcalibur (Thermo Fisher Scientific) was used to get the peak area for all the PC species and the internal standard. The internal standard calibration curve of PC-36:0 was used to calculate the relative concentration of all the PC lipid species in the samples.

Biliary PC analysis

Bile was isolated from the gallbladders of mice after killing. The bile was used to measure total PC per the manufacturer's instructions (MAK049; Sigma).

Quantification of mitochondrial DNA

Genomic DNA was extracted using DNAzol (Thermo Fisher Scientific) per the manufacturer's instructions. qPCR was performed on *Cox1* mitochondrial DNA and normalized to a nuclear *28S* sequence (20). The sequences of these primer sets are listed in **Supplemental Table 1**.

qPCR

We measured the mRNA expression of several genes involved in fatty acid uptake and synthesis [sterol response element binding protein 1c (*Srebp1c*), *Cd36*, and *Fas*], β-oxidation [acetyl-CoA carboxylase (*Acc*), acyl-CoA oxidase 1 (*Acox1*), carnitine palmitoyltransferase 1A (*Cpt1α*)], mitochondrial metabolism (*Pgc1a*), triglyceride production and secretion (*Dgat1*, *Dgat2*, and *Mtp*), cholesterol uptake and synthesis [*Hmgcs*, 3-hydroxy-3-methyl-glutaryl-coenzyme A reductase (*Hmgcr*), squalene epoxidase (*Sqle*), *Srebp2*, and LDL receptor (*Ldlr*)], inflammation (*Il1a*, *Il1b*, and *Tnfa*), and choline metabolism [*Pemt*, *Chdh*, *Bhmt*, *Chka*, solute carrier family 44 member 1 (*Slc44a1*), *Pld1*, *Chpt1*, *Pcyt1a*]. Total RNA was isolated from mouse liver using TRIzol Reagent (Ambion by Life Technologies) and qPCR was performed using gene-specific primers and the Applied Biosystems 7500 Real-Time PCR System as described previously (20, 21). Expressions of mRNA levels were calculated based on the ΔΔ-CT method and were normalized to 18S. Primer sequences are listed in Supplemental Table 1.

Plasma alanine aminotransferase and aspartate aminotransferase assays

Plasma was used to analyze aspartate aminotransferase (AST) and alanine aminotransferase (ALT) concentrations using enzymatic assays (Sekisui Diagnostics).

Plasma lipid analysis

Plasma lipid analyses were conducted as described previously (17). Total plasma triacylglycerol concentrations (L-Type TG M; Wako Diagnostics) and total plasma cholesterol concentrations were quantified enzymatically (Infinity Cholesterol Reagent; Thermo Fisher Scientific).

Calculation of tumor area

Total livers were collected and separated into the 4 major lobes (median, left, right, and caudal lobes). Professional images were taken from a dorsal and ventral perspective from the Cleveland Clinic's photography

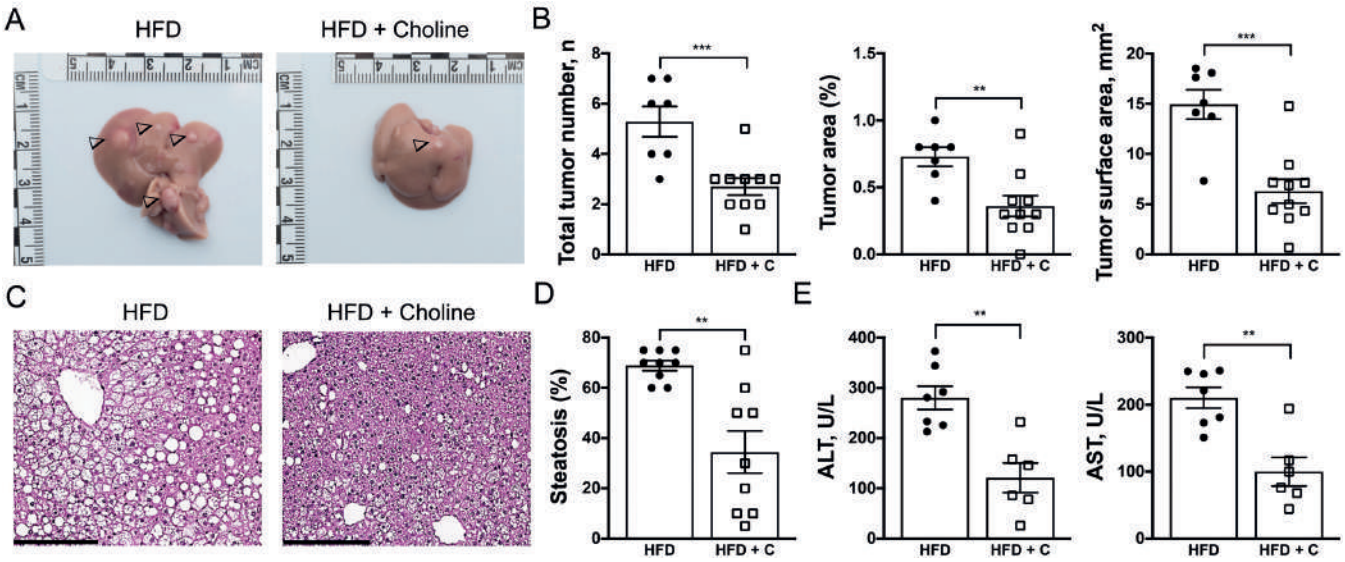

FIGURE 2 Dietary choline supplementation protects mice against HFD-induced HCC and hepatic steatosis. Representative images of whole livers with the triangles highlighting visible tumors (A), total tumor number (B; left panel), percentage of tumor area (B; middle panel), total tumor surface area (B; right panel) ($n = 7$–10), representative liver hematoxylin and eosin stains (C), percentage steatosis scores (D) ($n = 9$), and plasma ALT (E; left) and AST (E; right) ($n = 6$–7) measured in mice fed an HFD and an HFD+C for 30 wk. All data are presented as means ± SEMs. A 2-tailed Student's t test was used in panels B (left and right) and E. A Mann–Whitney rank sum test was used in panels B (middle) and D. $^{**}P \leq 0.01$; $^{***}P \leq 0.001$. Scale bar = 200 μm. ALT, alanine aminotransferase; AST, aspartate aminotransferase; HCC, hepatocellular carcinoma; HFD, high-fat diet; HFD+C, high-fat diet with supplemental choline.

core. The surface areas were calculated by drawing around each tumor and liver lobe, using both a ventral and dorsal view, with the use of ImageJ software (NIH).

Whole-blood flow cytometry

Peripheral blood was obtained at either 15 or 30 wk by submandibular venipuncture for circulating leukocyte analysis. Total white blood cell counts were performed using a hemocytometer following dilution in Turk's solution (catalog no. 8850-16; RICCA Chemical Company). RBCs were removed from flow cytometry preparations by treatment with BD Pharm Lyse, an ammonium chloride–based lysing buffer (catalog no. 555899; BD Biosciences). The remaining white blood cells were incubated with combinations of the following monoclonal antibodies: CD3e-APC-Cy7 clone 145-2C11 (BioLegend), CD4-Alexa Fluor 700 clone RM4-5 (BioLegend), CD8a-PE-Cy7 clone 53-6.7 (eBioscience), CD115-PE clone AFS98 (eBioscience), Ly-6G-APC clone 1A8 (eBioscience), and Ly-6C-FITC clone AL-21 (BD Biosciences). Data were acquired on a BD LSRII instrument (BD Biosciences) and analyzed using FlowJo Data Analysis Software version 10.0.8 (FlowJo LLC). Immune cell populations were analyzed using the following gating techniques: myeloid-derived suppressor cells (MDSCs; $Ly6G^{-}CD115^{+}Lys6C^{high}$), T lymphocytes ($CD19^{-}CD3^{+}$), T-helper cells ($CD19^{-}CD3^{+}CD4^{+}$), cytotoxic T cells ($CD19^{-}CD3^{+}CD8^{+}$), B lymphocytes ($CD19^{+}CD3^{-}$), monocytes ($CD115^{+}Ly6G^{-}$), and neutrophils ($Ly6G^{+}CD115^{-}$).

Statistical analysis

All statistical analyses were performed using Graphpad Prism, and $P < 0.05$ was considered statistically significant. All data are presented as means ± SEMs unless otherwise noted in the figure legends. All data were tested for equal variance and normality. For 2-group comparison of parametric data, a 2-tailed Student's t test was performed, whereas nonparametric data were analyzed with a Mann–Whitney rank sum test. All measures with repeated analysis examined over time were conducted using a repeated-measures 2-factor ANOVA with Holm–Sidak post-hoc analysis.

Results

Choline supplementation reduces body weight and liver weight when fed a HFD

In humans, ingestion of a choline-rich meal (~500 mg) increases circulating choline concentrations by ~100% at 1–2 h after consumption (14). Plasma choline concentrations increased by 52% (35 μM compared with 23 μM) in HFD+C-fed mice relative to the HFD control mice (**Figure 1**A). Mice fed the choline-supplemented diet exhibited an 88% increase in circulating betaine concentrations (54 μM compared with 29 μM in the HFD-fed mice; Figure 1B). Mice fed an HFD+C gained less weight than their HFD-fed counterparts beginning at week 15 until the end of the study, resulting in a 10.2% overall decrease in body weight at 30 wk (Figure 1C, D). Mice fed the HFD+C had decreased liver weight (Figure 1E, F), with no changes in spleen or adipose tissue weight between the 2 dietary groups (**Supplemental Figure 1**A–D).

It has been well documented that patients with chronic liver disease develop glucose tolerance and insulin resistance (22). Mice fed an HFD+C had greater plasma glucose concentrations 30 min after the initial glucose injection compared with mice fed an HFD alone (Figure 1G). Despite that increase, both groups of mice returned to similar baseline concentrations at 120 min. AUC analysis demonstrated that glucose tolerance was similar between the 2 dietary groups (Figure 1H). Collectively, these data suggest that mice fed an HFD+C are leaner and have decreases in liver mass compared with HFD-fed mice.

Dietary choline slows HCC progression and alleviates hepatic steatosis

Given the fact that mice fed an HFD+C had decreases in liver mass, we wanted to assess the overall tumor burden in these mice. Mice fed an HFD+C exhibited less tumor burden in the liver (**Figure 2**A, B) accompanied by attenuated hepatic lipid drop accumulation (Figure 2C) compared with the

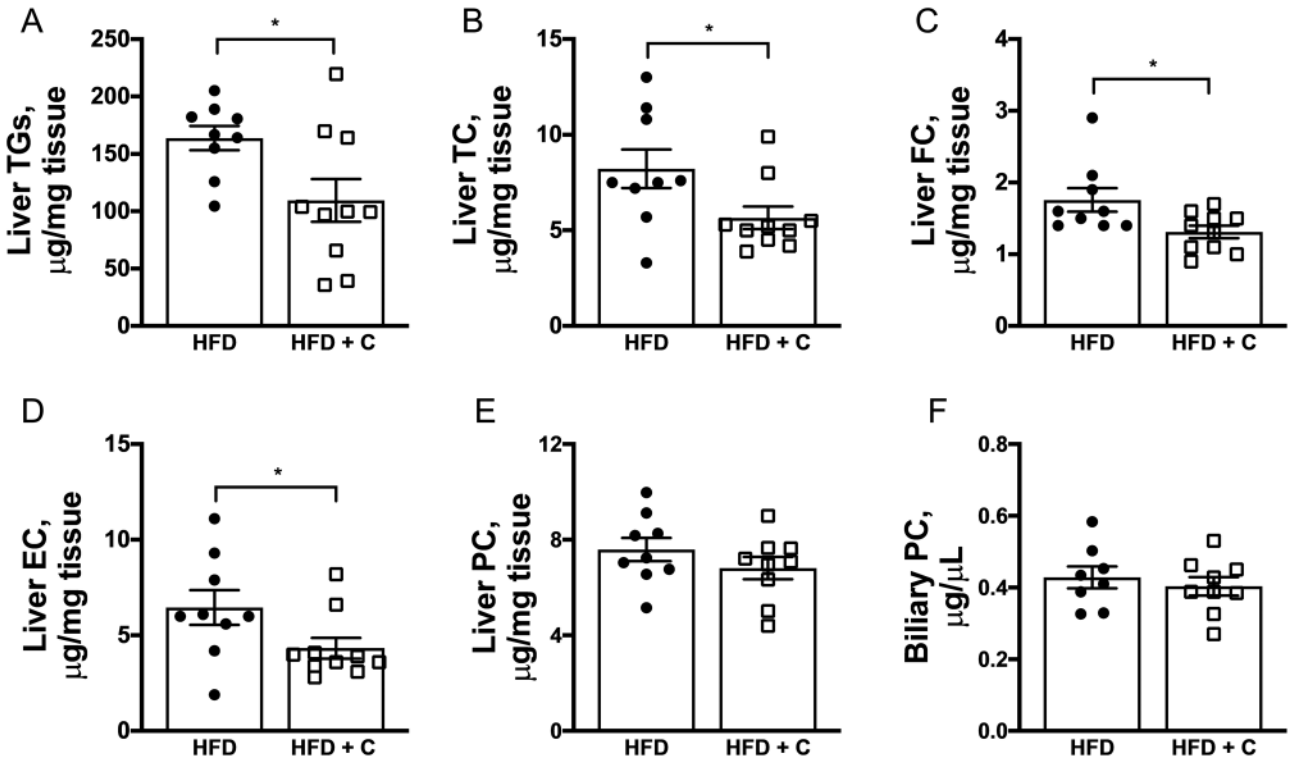

FIGURE 3 Dietary choline supplementation protects mice against HFD-induced hepatic steatosis. (A–F) Hepatic TGs (A), hepatic TC (B), hepatic FC (C), hepatic EC (D), hepatic total PC (E), and biliary PC (F) were measured in mice fed an HFD and an HFD+C for 30 wk ($n = 8$–10). All data are presented as means ± SEMs. A 2-tailed Student's t test was used in panels A, B, D, E, and F. A Mann–Whitney rank sum test was used in panel C. $^*P \leq 0.05$. EC, esterified cholesterol; FC, free cholesterol; HFD, high-fat diet; HFD+C, high-fat diet with supplemental choline; PC, phosphatidylcholine; TC, total cholesterol; TG, triglyceride.

HFD-fed mice. Mice fed an HFD+C had a 50% decrease in hepatic steatosis (Figure 2D), exhibited lower ALT and AST concentrations (Figure 2E), and had reductions in triglycerides, total cholesterol, free cholesterol, and esterified cholesterol in the liver compared with HFD-fed mice (**Figure 3**A–D). Mice fed an HFD+C did not exhibit alterations in total hepatic PC concentrations (Figure 3E), but did display small decreases in certain PC species, such as 34:1 PC, 36:1 PC, 38:3 PC, and 38:0 PC (**Supplemental Figure 2**). Further, mice did not display significant alterations in total biliary PC concentrations (Figure 3F). Mice fed an HFD+C had lower plasma cholesterol and tended to have lower plasma triglycerides ($P = 0.08$) compared with those fed an HFD (**Supplemental Figure 3**).

Dietary choline alters lipid metabolism gene expression and increases mitochondrial DNA abundance in the liver

Mice fed an HFD+C exhibited less tumor burden and hepatic steatosis (Figure 2) than the HFD-fed mice, yet the mechanism(s) behind this are poorly understood. Choline supplementation increased the mRNA expression of *Cpt1a* and *Pgc1a* (**Figure 4**A, C), whereas *Acox1* expression tended to increase ($P = 0.09$; Figure 4B). Further, the numbers of mitochondria were elevated in livers from choline-fed mice (Figure 4D). The mRNA expressions of genes involved in cholesterol uptake and synthesis (*Ldlr*, *Hmgcr*, and *Srebp2*) were also greater in mice fed a choline diet (**Table 1**). Collectively, these data suggest that choline feeding increases mitochondrial density and associated fat oxidation gene expression in the liver.

Choline supplementation nearly eliminates circulating MDSCs

Hepatic inflammation can directly contribute to the progression of HCC (23). The HFD+C did not affect lobular inflammation or ballooning degeneration in the liver (**Supplemental Table 2**). Consistently, there were no differences in proinflammatory gene expression between the 2 groups of mice (Table 1). Collectively, these data demonstrate that HFD+C-fed mice are protected against diet-induced HCC tumor burden and hepatic steatosis while exhibiting no differences in hepatic inflammation.

Despite the lack of changes in hepatic inflammation in mice fed an HFD+C, we wanted to determine if choline feeding could influence circulating immune cell populations. Choline supplementation significantly decreased circulating MDSCs (**Figure 5**A), T lymphocytes (Figure 5B–D), monocytes (**Supplemental Figure 4**), and neutrophils (Supplemental Figure 4) at 15 wk of feeding. Other circulating immune cell populations, such as B lymphocytes (Supplemental Figure 4), were unchanged at this time point. Interestingly, both the HFD- and HFD+C-fed mice displayed similar concentrations of MDSCs, T lymphocytes, B lymphocytes, monocytes, and neutrophils (**Supplemental Figure 5**) at 30 wk of feeding. Collectively, these results suggest that choline supplementation decreases circulating MDSCs early in the progression of HCC, which may contribute to the protection observed in these supplemented animals.

Discussion

Choline deficiency has been widely studied in hepatic steatosis, hepatic inflammation, and to a lesser extent, in HCC

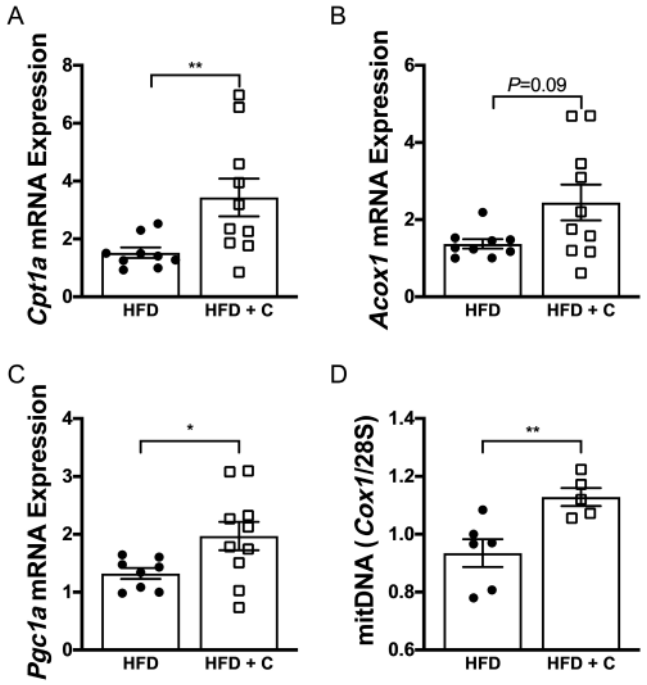

FIGURE 4 Choline supplementation increased fat oxidation gene expression and mitochondria abundance in the liver. (A–D) mRNA expression of *Cpt1a* (A), *Acox1* (B), and *Pgc1a* (C) (n = 8–10) and mitochondrial DNA levels of *Cox1* (D) (n = 5–6) was measured in livers from mice fed an HFD or an HFD+C for 30 wk. All data are presented as means ± SEMs. A 2-tailed Student's t test was used in panel D. A Mann–Whitney rank sum test was used in panel A, B, and C. $^{*}P \leq 0.05$; $^{**}P \leq 0.01$. RNA expression levels are normalized to the housekeeping gene, *18S*, and are presented as fold change. *Acox1*, acyl-CoA oxidase 1; *Cox1*, cyclooxygenase 1; *Cpt1a*, carnitine palmitoyltransferase 1A; HFD, high-fat diet; HFD+C, high-fat diet with supplemental choline; mitDNA, mitochondrial DNA; *Pgc1a*, peroxisome proliferator-activated receptor γ coactivator 1α.

TABLE 1 Hepatic mRNA expression of genes involved in lipid and choline metabolism and inflammation[1]

Gene	HFD	HFD+C	*P*
Srebp1c	1.10 ± 0.36	1.75 ± 1.12	0.13[2]
Cd36	2.11 ± 1.15	2.81 ± 1.82	0.34[3]
Fas	0.60 ± 0.29	0.75 ± 0.34	0.34[3]
Acc	1.22 ± 0.34	1.39 ± 0.70	0.52[3]
Dgat1	1.81 ± 0.53	3.21 ± 1.96	0.11[2]
Dgat2	1.76 ± 1.14	1.89 ± 0.93	0.44[2]
Mttp	1.98 ± 0.91	3.97 ± 2.62	0.045[3]
Hmgcs	2.49 ± 1.04	4.33 ± 2.70	0.07[3]
Hmgcr	2.25 ± 1.01	6.30 ± 4.75	0.010[2]
Sqle	2.35 ± 1.16	3.23 ± 2.07	0.28[3]
Srebp2	1.44 ± 0.50	2.50 ± 1.28	0.043[2]
Ldlr	1.38 ± 0.40	2.51 ± 1.44	0.035[2]
Il1a	1.15 ± 0.77	1.52 ± 1.09	0.39[2]
Il1b	1.80 ± 1.37	1.98 ± 1.40	0.90[2]
Tnfa	1.94 ± 0.77	1.57 ± 0.79	0.32[3]
Pemt	0.87 ± 0.36	0.96 ± 0.48	0.69[3]
Chdh	0.75 ± 0.23	1.63 ± 1.55	0.16[2]
Bhmt	1.35 ± 1.00	2.75 ± 2.94	0.21[2]
Chka	1.05 ± 0.41	1.20 ± 0.51	0.51[3]
Slc44a1	0.77 ± 0.51	0.43 ± 0.21	0.11[2]
Pld1	1.07 ± 0.40	2.25 ± 1.72	0.13[2]
Chpt1	0.79 ± 0.45	0.80 ± 0.42	0.91[2]
Pcyt1	2.17 ± 1.44	2.90 ± 2.32	0.60[2]

[1] Values are means ± SDs; n = 8–10. RNA expression levels were normalized to the housekeeping gene, *18S*, and are presented as fold change. *Acc*, acetyl-CoA carboxylase; *Bhmt*, betaine-homocysteine *S*-methyltransferase; *Cd36*, cluster of differentiation 36; *Chdh*, choline dehydrogenase; *Chka*, choline kinase α; *Chpt1*, choline phosphotransferase 1; *Dgat1*, diacylglycerol *O*-acyltransferase 1; *Dgat2*, diacylglycerol *O*-acyltransferase 2; *Fas*, fatty acid synthase; HFD, high-fat diet; HFD+C, high-fat diet with supplemental choline; *Hmgcr*, 3-hydroxy-3-methylglutaryl-CoA reductase; *Hmgcs*, 3-hydroxy-3-methylglutaryl-CoA synthase; *Il1a*, IL-1α; *Il1b*, IL-1β; *Ldlr*, LDL receptor; *Mttp*, microsomal triglyceride transfer protein; *Pcyt1a*, choline-phosphate cytidylyltransferase A; *Pemt*, phosphatidylethanolamine *N*-methyltransferase; *Pld1*, phospholipase D1; *Slc44a1*, solute carrier family 44 member 1; *Sqle*, squalene epoxidase; *Srebp1c*, sterol regulatory element binding transcription factor 1c; *Srebp2*, sterol regulatory element-binding protein 2; *Tnfa*, TNF-α.
[2] Mann–Whitney rank sum test used.
[3] Two-tailed Student's t test used.

(24, 25). However, less is known about choline supplementation in this context. To our knowledge, this is the first work to identify choline supplementation as a protective mechanism in a model of HFD-driven HCC. The data herein point to 2 potential mechanisms that may contribute to the protection against HCC. First, mice fed an HFD+C exhibited increases in gene expression associated with fat oxidation and had elevated mitochondrial abundance in the liver. Second, choline supplementation significantly decreased MDSCs after 15 wk of diet feeding. This work highlights the importance of choline metabolism in the etiology of HCC. Further work is warranted to elucidate the precise mechanisms that contribute to this protection.

MDSCs are a population of myeloid immune cells whose unifying feature is their ability to suppress T-cell function (26). They are found enriched in the circulation of cancer patients and track with disease response to chemotherapeutic interventions. Circulating MDSC concentrations can predict which individuals will respond to immunotherapy-based approaches, and depletion of these cells can have substantial antitumor effects (27). Furthermore, circulating MDSCs track with tumor progression but not with liver fibrosis or inflammation (28). Of note, we showed that MDSCs were 95% lower in mice fed supplemental choline, which may have contributed to the overall reduction in tumor burden in this group. Furthermore, HFD+C-fed mice had significantly reduced circulating $CD3^+$ T cells, including both $CD4^+$ T-helper cells and $CD8^+$ cytotoxic T cells. While this may be a reflection of reduced carcinogenesis at 15 wk, it may have contributed mechanistically to our observed results. For example, in a similar model of carcinogen-induced murine HCC, it was noted that T cells (primarily cytotoxic $CD8^+$) prevented initial tumor formation (29). Thus, it is possible that HFD+C-fed mice had an accumulation of intrahepatic T cells at 15 wk, resulting in an overall reduction in circulating T cells in this group. Importantly, $CD4^+$ T-helper cells have been described as critical to NAFLD-associated hepatocarcinogenesis (30). These studies attributed increased mitochondrial oxidative stress to fatty state of the liver, which leads to the selective loss of $CD4^+$ T-helper cells. As such, it is important to recognize that our model of HFD-driven HCC accumulates both cytotoxic T cells and T-helper cells in the liver to contribute to the pathogenesis of HCC. Finally, regarding the contribution of the immune system in this model, a role for choline in the inflammatory response of macrophages has recently been described (31, 32). It is interesting to note that reduced choline uptake from macrophages alters their mitochondrial lipid content and leads to a reduction in the secretion of proinflammatory cytokines. By supplying ample

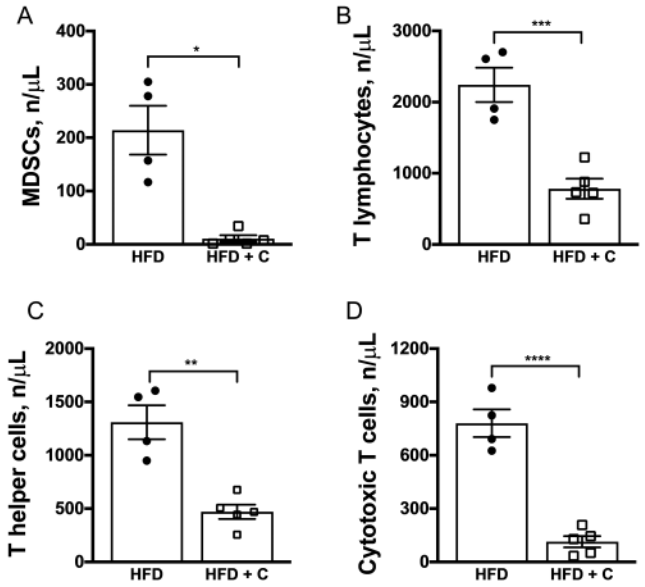

FIGURE 5 Mice fed an HFD±C for 15 wk exhibit a reduction in circulating MDSCs and T lymphocytes. (A–D) Blood was isolated to measure circulating MDSCs (A), T lymphocytes (B), T-helper cells (C), and cytotoxic T cells (D) at 15 wk of HFD or HFD+C feeding. All data are presented as means ± SEMs ($n = 4$–5). A 2-tailed Student's t test was used in panels B, C, and D. A Mann–Whitney rank sum test was used in panel A. $^{*}P \leq 0.05$; $^{**}P \leq 0.01$; $^{***}P \leq 0.001$; $^{****}P \leq 0.0001$. HFD, high-fat diet; HFD+C, high-fat diet with supplemental choline; MDSC, myeloi- derived suppressor cell.

choline in our dietary model, we may have promoted the antitumor effects of intrahepatic macrophages and partially ameliorated HFD-driven HCC.

Hepatic steatosis is clinically defined as intrahepatic fat of ≥5% of liver weight (33). Prolonged accumulation of lipids in the liver may lead to metabolic dysfunction, inflammation, and advanced forms of NAFLD (33). There are several perturbed mechanisms that may contribute to an accumulation of hepatic lipids, including reduced β-oxidation, reduced VLDL secretion, increased fatty acid influx, and increased de-novo lipogenesis (33). In mice fed an HFD+C, we observed a significant decrease in the accumulation of lipids in the liver. To attempt to identify the mechanisms that may contribute to this protection, we analyzed the expression of genes involved in the aforementioned mechanisms. Interestingly, choline supplementation increased the expression of genes involved in β-oxidation. Both of these genes, *Acox1* and *Cpt1a*, have been identified as direct targets of the master regulator of hepatic lipid metabolism, peroxisome proliferator-activated receptor α (*Pparα*) (34). We also observed a significant increase in the PPAR-γ coactivator 1α (*Pgc1a*), which is important in coactivating fatty acid oxidation genes in coordination with *Pparα* (35). Other groups have recently identified a choline metabolite [1-palmitoyl-2-oleoly-*sn*-glycerol-3-phosphocholine (16:0/18:1-GPC)] as a ligand of PPARα (36). Chakravarthy et al. (36) directly infused this lipid into the portal vein of mice, inducing PPARα gene expression and reducing hepatic steatosis. In accordance with this previous work from Chakravarthy et al., we initially speculated that choline supplementation would increase 16:0/18:1-GPC concentrations in the liver and thereby contribute to the protection against HFD-induced fatty liver. We went on to measure 40 PC species and found none that were significantly increased with choline feeding. Similarly, we also measured total biliary PC since perturbations in biliary PC secretion can lead to HCC in mice (37). Mice fed an HFD+C exhibited no differences in biliary PC concentrations compared with the HFD-fed control group. Collectively, our results suggest that there are no differences in the total pool of hepatic or biliary PC concentrations, thereby making this an unlikely mechanism contributing to the increase in fat oxidation gene expression in the liver.

To assess the mechanism coordinating increases in mitochondrial DNA content and fat oxidation gene expression in the liver, we measured circulating betaine (an oxidative product of choline). Interestingly, high dietary intakes of betaine and choline are associated with a lower risk of primary liver cancer (38). Further, betaine treatment in a human hepatic cell line attenuated lipid accumulation, increased mitochondrial DNA content and activity, and increased the expression of genes involved in fatty acid oxidation (39). We discovered that mice fed a choline-supplemented diet had significantly elevated circulating betaine concentrations. It is plausible that the increases in mitochondrial DNA content and fatty acid oxidation gene expression are directly related to betaine metabolism; however, more work is required to further elucidate these mechanisms.

Aside from the protection against HFD-induced triglyceride accumulation in the liver, mice fed an HFD+C also exhibited a reduction in hepatic cholesterol concentrations compared with HFD-fed mice. One of the master regulators of cholesterol metabolism in the liver is *Srebp2*. SREBP2 is activated when hepatic cholesterol concentrations are low, acting as a feedback regulator in an attempt to further increase cholesterol concentrations in the liver (40). Two notorious SREBP2 target genes are *Ldlr* and *Hmgcr* enzymes (40). In mice fed an HFD+C for 30 wk, the hepatic expression of *Srebp2*, *Ldlr*, and *Hmgcr* were all elevated compared with an HFD alone. Mice fed supplemental choline likely exhibit increases in the expression of these sterol-response genes as a feedback mechanism to further increase hepatic cholesterol concentrations, similar to the HFD-fed group; however, this would need to be investigated further.

The tumor microenvironment is made up of hepatic stellate cells, fibroblasts, immune cells, and endothelial cells (41). Recent work has attempted to identify global gene expression patterns within the HCC tumor microenvironment (42–46). Interestingly, cancer cells have been demonstrated to display aberrant choline and lipid metabolism (47). For example, a reduction in choline kinase *a* expression, which catalyzes the first step in PC synthesis, has been demonstrated to reduce cell proliferation in breast cancer cells and tissues (47–50). The major limitation to this study is our inability to assess gene expression changes between tumor and adjacent nontumor samples as they relate to choline and lipid metabolism. In an attempt to overcome this limitation, we analyzed the expression of genes involved in choline metabolism using visible nontumor liver tissue between the 2 groups of mice. Of all the genes analyzed, none were significantly dysregulated in mice fed an HFD+C. It is worth noting that the choline transporter, *Slc44a1*, and phospholipase D1 (*Pld1*) tended ($P = 0.10$) to decrease and increase, respectively, compared with HFD-fed control mice. Further studies are warranted to fully understand the impact choline supplementation has on the tumor microenvironment in HCC.

In conclusion, this work demonstrates that choline supplementation protects mice against liver cancer in the setting of HFD feeding. Mechanistically, these mice may be protected

against HFD-induced liver cancer by increasing fat oxidation in the liver and by reducing the number of circulating MDSCs; however, more work is needed to elucidate the exact mechanisms that are contributing to this protection.

Acknowledgments

The authors acknowledge Zeneng Wang for his technical assistance to this work. The authors' responsibilities were as follows—RNH: designed the study and has primary responsibility for the final content; ALB, KC, ADG, RZ, CN, DSA, and RNH: conducted research; ALB, KC, and RNH: analyzed the data and wrote the manuscript; APO and MT: critically reviewed the manuscript and provided resources necessary to complete experiments; and all authors: read and approved the final manuscript.

References

1. Bray F, Ferlay J, Soerjomataram I, Siegel RL, Torre LA, Jemal A. Global cancer statistics 2018: GLOBOCAN estimates of incidence and mortality worldwide for 36 cancers in 185 countries. CA Cancer J Clin 2018;68(6):394–424.
2. Coskun M. Hepatocellular carcinoma in the cirrhotic liver: evaluation using computed tomography and magnetic resonance imaging. Exp Clin Transplant 2017;15(Suppl 2):36–44.
3. Goossens N, Sun X, Hoshida Y. Molecular classification of hepatocellular carcinoma: potential therapeutic implications. Hepat Oncol 2015;2(4):371–9.
4. Kornberg A. Liver transplantation for hepatocellular carcinoma beyond Milan criteria: multidisciplinary approach to improve outcome. ISRN Hepatol 2014;2014:706945.
5. Zeisel SH. Choline: critical role during fetal development and dietary requirements in adults. Annu Rev Nutr 2006;26:229–50.
6. Mehedint MG, Zeisel SH. Choline's role in maintaining liver function: new evidence for epigenetic mechanisms. Curr Opin Clin Nutr Metab Care 2013;16(3):339–45.
7. da Costa KA, Garner SC, Chang J, Zeisel SH. Effects of prolonged (1 year) choline deficiency and subsequent re-feeding of choline on 1,2-*sn*-diradylglycerol, fatty acids and protein kinase C in rat liver. Carcinogenesis 1995;16(2):327–34.
8. Ghoshal AK, Farber E. The induction of liver cancer by dietary deficiency of choline and methionine without added carcinogens. Carcinogenesis 1984;5(10):1367–70.
9. Locker J, Reddy TV, Lombardi B. DNA methylation and hepatocarcinogenesis in rats fed a choline-devoid diet. Carcinogenesis 1986;7(8):1309–12.
10. Buchman AL, Ament ME, Sohel M, Dubin M, Jenden DJ, Roch M, Pownall H, Farley W, Awal M, Ahn C. Choline deficiency causes reversible hepatic abnormalities in patients receiving parenteral nutrition: proof of a human choline requirement: a placebo-controlled trial. JPEN J Parenter Enteral Nutr 2001;25(5):260–8.
11. Yoshimoto S, Loo TM, Atarashi K, Kanda H, Sato S, Oyadomari S, Iwakura Y, Oshima K, Morita H, Hattori M, et al. Obesity-induced gut microbial metabolite promotes liver cancer through senescence secretome. Nature 2013;499(7456):97–101.
12. Niwa Y, Ishikawa K, Ishigami M, Honda T, Achiwa K, Izumoto T, Maekawa R, Hosokawa K, Iida A, Seino Y, et al. Effect of hyperglycemia on hepatocellular carcinoma development in diabetes. Biochem Biophys Res Commun 2015;463(3):344–50.
13. Takemura N, Hagio M, Ishizuka S, Ito H, Morita T, Sonoyama K. Inulin prolongs survival of intragastrically administered Lactobacillus plantarum no. 14 in the gut of mice fed a high-fat diet. J Nutr 2010;140(11):1963–9.
14. Tang WH, Wang Z, Levison BS, Koeth RA, Britt EB, Fu X, Wu Y, Hazen SL. Intestinal microbial metabolism of phosphatidylcholine and cardiovascular risk. N Engl J Med 2013;368(17):1575–84.
15. Wang Z, Klipfell E, Bennett BJ, Koeth R, Levison BS, Dugar B, Feldstein AE, Britt EB, Fu X, Chung YM, et al. Gut flora metabolism of phosphatidylcholine promotes cardiovascular disease. Nature 2011;472(7341):57–63.
16. Brown JM, Chung S, Sawyer JK, Degirolamo C, Alger HM, Nguyen T, Zhu X, Duong MN, Wibley AL, Shah R, et al. Inhibition of stearoyl-coenzyme A desaturase 1 dissociates insulin resistance and obesity from atherosclerosis. Circulation 2008;118(14):1467–75.
17. Gromovsky AD, Schugar RC, Brown AL, Helsley RN, Burrows AC, Ferguson D, Zhang R, Sansbury BE, Lee RG, Morton RE, et al. Delta-5 fatty acid desaturase FADS1 impacts metabolic disease by balancing proinflammatory and proresolving lipid mediators. Arterioscler Thromb Vasc Biol 2018;38(1):218–31.
18. Helsley RN, Venkateshwari V, Brown AL, Gromovsky AD, Schugar RC, Ramachandiran I, Fung K, Kabbany MN, Banerjee R, Neumann CK, et al. Obesity-linked suppression of membrane-bound *O*-acyltransferase 7 (MBOAT7) drives non-alcoholic fatty liver disease. Elife 2019;8:e49882.
19. Lee RG, Kelley KL, Sawyer JK, Farese RV, Jr, Parks JS, Rudel LL. Plasma cholesteryl esters provided by lecithin:cholesterol acyltransferase and acyl-coenzyme a:cholesterol acyltransferase 2 have opposite atherosclerotic potential. Circ Res 2004;95(10):998–1004.
20. Helsley RN, Sui Y, Park SH, Liu Z, Lee RG, Zhu B, Kern PA, Zhou C. Targeting IkappaB kinase beta in adipocyte lineage cells for treatment of obesity and metabolic dysfunctions. Stem Cells 2016;34(7):1883–95.
21. Lord CC, Ferguson D, Thomas G, Brown AL, Schugar RC, Burrows A, Gromovsky AD, Betters J, Neumann C, Sacks J, et al. Regulation of hepatic triacylglycerol metabolism by CGI-58 does not require ATGL co-activation. Cell Rep 2016;16(4):939–49.
22. Han H, Zhang T, Jin Z, Guo H, Wei X, Liu Y, Chen Q, He J. Blood glucose concentration and risk of liver cancer: systematic review and meta-analysis of prospective studies. Oncotarget 2017;8(30):50164–73.
23. Yu LX, Ling Y, Wang HY. Role of nonresolving inflammation in hepatocellular carcinoma development and progression. NPJ Precis Oncol 2018;2(1):6.
24. Caballero F, Fernandez A, Matias N, Martinez L, Fucho R, Elena M, Caballeria J, Morales A, Fernandez-Checa JC, Garcia-Ruiz C. Specific contribution of methionine and choline in nutritional nonalcoholic steatohepatitis: impact on mitochondrial *S*-adenosyl-L-methionine and glutathione. J Biol Chem 2010;285(24):18528–36.
25. Kishida N, Matsuda S, Itano O, Shinoda M, Kitago M, Yagi H, Abe Y, Hibi T, Masugi Y, Aiura K, et al. Development of a novel mouse model of hepatocellular carcinoma with nonalcoholic steatohepatitis using a high-fat, choline-deficient diet and intraperitoneal injection of diethylnitrosamine. BMC Gastroenterol 2016;16(1):61.
26. Veglia F, Perego M, Gabrilovich D. Myeloid-derived suppressor cells coming of age. Nat Immunol 2018;19(2):108–19.
27. Highfill SL, Cui Y, Giles AJ, Smith JP, Zhang H, Morse E, Kaplan RN, Mackall CL. Disruption of CXCR2-mediated MDSC tumor trafficking enhances anti-PD1 efficacy. Sci Transl Med 2014;6(237):237ra67.
28. Arihara F, Mizukoshi E, Kitahara M, Takata Y, Arai K, Yamashita T, Nakamoto Y, Kaneko S. Increase in CD14+HLA-DR -/low myeloid-derived suppressor cells in hepatocellular carcinoma patients and its impact on prognosis. Cancer Immunol Immunother 2013;62(8):1421–30.
29. Schneider C, Teufel A, Yevsa T, Staib F, Hohmeyer A, Walenda G, Zimmermann HW, Vucur M, Huss S, Gassler N, et al. Adaptive immunity suppresses formation and progression of diethylnitrosamine-induced liver cancer. Gut 2012;61(12):1733–43.
30. Ma C, Kesarwala AH, Eggert T, Medina-Echeverz J, Kleiner DE, Jin P, Stroncek DF, Terabe M, Kapoor V, ElGindi M, et al. NAFLD causes selective CD4(+) T lymphocyte loss and promotes hepatocarcinogenesis. Nature 2016;531(7593):253–7.
31. Sanchez-Lopez E, Zhong Z, Stubelius A, Sweeney SR, Booshehri LM, Antonucci L, Liu-Bryan R, Lodi A, Terkeltaub R, Lacal JC, et al. Choline uptake and metabolism modulate macrophage IL-1beta and IL-18 production. Cell Metab 2019;29(6):1350–62.e7.
32. Snider SA, Margison KD, Ghorbani P, LeBlond ND, O'Dwyer C, Nunes JRC, Nguyen T, Xu H, Bennett SAL, Fullerton MD. Choline transport links macrophage phospholipid metabolism and inflammation. J Biol Chem 2018;293(29):11600–11.
33. Nassir F, Rector RS, Hammoud GM, Ibdah JA. Pathogenesis and prevention of hepatic steatosis. Gastroenterol Hepatol (NY) 2015;11(3):167–75.
34. Rakhshandehroo M, Knoch B, Muller M, Kersten S. Peroxisome proliferator-activated receptor alpha target genes. PPAR Res 2010;2010:1–20.

35. Vega RB, Huss JM, Kelly DP. The coactivator PGC-1 cooperates with peroxisome proliferator-activated receptor alpha in transcriptional control of nuclear genes encoding mitochondrial fatty acid oxidation enzymes. Mol Cell Biol 2000;20(5):1868–76.
36. Chakravarthy MV, Lodhi IJ, Yin L, Malapaka RR, Xu HE, Turk J, Semenkovich CF. Identification of a physiologically relevant endogenous ligand for PPARalpha in liver. Cell 2009;138(3):476–88.
37. Katzenellenbogen M, Mizrahi L, Pappo O, Klopstock N, Olam D, Jacob-Hirsch J, Amariglio N, Rechavi G, Domany E, Galun E, et al. Molecular mechanisms of liver carcinogenesis in the mdr2-knockout mice. Mol Cancer Res 2007;5(11):1159–70.
38. Zhou RF, Chen XL, Zhou ZG, Zhang YJ, Lan QY, Liao GC, Chen YM, Zhu HL. Higher dietary intakes of choline and betaine are associated with a lower risk of primary liver cancer: a case-control study. Sci Rep 2017;7(1):679.
39. Zhang L, Qi Y, Z ALuo, Liu S, Zhang Z, Zhou L. Betaine increases mitochondrial content and improves hepatic lipid metabolism. Food Funct 2019;10(1):216–23.
40. Brown MS, Goldstein JL. The SREBP pathway: regulation of cholesterol metabolism by proteolysis of a membrane-bound transcription factor. Cell 1997;89(3):331–40.
41. Yang JD, Nakamura I, Roberts LR. The tumor microenvironment in hepatocellular carcinoma: current status and therapeutic targets. Semin Cancer Biol 2011;21(1):35–43.
42. Chen X, Cheung ST, So S, Fan ST, Barry C, Higgins J, Lai KM, Ji J, Dudoit S, Ng IO, et al. Gene expression patterns in human liver cancers. Mol Biol Cell 2002;13(6):1929–39.
43. Dong H, Zhang L, Qian Z, Zhu X, Zhu G, Chen Y, Xie X, Ye Q, Zang J, Ren Z, et al. Identification of HBV-MLL4 integration and its molecular basis in Chinese hepatocellular carcinoma. PLoS One 2015;10(4):e0123175.
44. Kim JW, Wang XW. Gene expression profiling of preneoplastic liver disease and liver cancer: a new era for improved early detection and treatment of these deadly diseases? Carcinogenesis 2003;24(3):363–9.
45. Lee JS, Heo J, Libbrecht L, Chu IS, Kaposi-Novak P, Calvisi DF, Mikaelyan A, Roberts LR, Demetris AJ, Sun Z, et al. A novel prognostic subtype of human hepatocellular carcinoma derived from hepatic progenitor cells. Nat Med 2006;12(4):410–6.
46. Lee JS, Thorgeirsson SS. Genome-scale profiling of gene expression in hepatocellular carcinoma: classification, survival prediction, and identification of therapeutic targets. Gastroenterology 2004;127(5 Suppl 1):S51–5.
47. Mori N, Wildes F, Takagi T, Glunde K, Bhujwalla ZM. The tumor microenvironment modulates choline and lipid metabolism. Front Oncol 2016;6:262.
48. Glunde K, Raman V, Mori N, Bhujwalla ZM. RNA interference-mediated choline kinase suppression in breast cancer cells induces differentiation and reduces proliferation. Cancer Res 2005;65(23):11034–43.
49. Krishnamachary B, Glunde K, Wildes F, Mori N, Takagi T, Raman V, Bhujwalla ZM. Noninvasive detection of lentiviral-mediated choline kinase targeting in a human breast cancer xenograft. Cancer Res 2009;69(8):3464–71.
50. Mori N, Glunde K, Takagi T, Raman V, Bhujwalla ZM. Choline kinase down-regulation increases the effect of 5-fluorouracil in breast cancer cells. Cancer Res 2007;67(23):11284–90.